ADVANCED MATERIALS

DOI: 10.1002/adma.200501832

Microstructure and Composition of Focused-Ion-Beam-Deposited Pt Contacts to GaN Nanowires**

By *Douglas Tham*, *Chang-Yong Nam*, and *John E. Fischer**

GaN is a technologically important semiconductor with a wide direct bandgap (3.39 eV), and boasts strong light emission in the blue and UV regions of the electromagnetic spectrum. It finds extensive commercial applications in lasers and light-emitting diodes.[1] Because of its high melting temperature, high breakdown field, and high saturation drift velocity, it is a prime candidate for high-temperature, high-voltage, and high-power optoelectronic-device applications. In recent years, research interest in GaN nanowires has increased significantly because, for sufficiently thin nanowires, quantum-confinement effects may be observed,[2] which may lead to novel behavior and applications. GaN nanowires appear to be especially attractive as low-dimensional high-power blue and UV laser light sources, because it is anticipated that high optical gains and low lasing thresholds will be achievable when the nanowire diameter is smaller than the exciton radius.[3] It has been demonstrated that GaN nanowires possess great potential for photonic-, optoelectronic-, and electronic-device applications.[4–7]

For practical device applications, nanowires have to be controllably assembled, precisely located, and individually contacted in order to build device architectures. This continues to be a formidable technical challenge. Traditional lithographic approaches are hindered by the need to register contacts to individual nanowires, although new methodologies to circumvent this limitation have been proposed.[8] Recently, direct writing techniques using focused ion beams (FIBs) have been used to form interconnects to individual nanowires.[9–13] To do this, an organoplatinum precursor gas flow was directed at the surface of the sample while the target region was irradiated with an energetic particle beam, which decomposed the gas and deposited Pt over the irradiated region. Decomposition of the precursor and Pt deposition can be achieved using focused beams of ions (IBID-Pt, where IBID = ion-beam-induced deposition)[9,10,12,13] or electrons (EBID-Pt, where EBID = electron-beam-induced deposition).[11] The unusually low resistance or ohmic contacts on n-type GaN nanowires[9] suggest that IBID-Pt contacts are different from conventional thin-film Pt contacts, which generally exhibit a large Schottky barrier on n-GaN. Here we present a complete investigation of the structural and chemical character of FIB-deposited metal contacts on GaN nanowires, in order to understand how composition and microstructure affect the electrical performance.

Contact structures have been traditionally studied using cross-sectional transmission electron microscopy (TEM). TEM enables imaging, diffraction, and spectroscopy at near-atomic spatial resolution on the same region of interest, providing a wealth of morphological, structural, and compositional information, so that even the most complex contact structures can be readily understood.[14,15] Although many preparation techniques are capable of creating cross-sections suitable for TEM imaging,[16,17] these generally offer little control over the region exposed for TEM observation and are, therefore, not useful for preparing cross-sections of our nanowire circuits. The so-called lift-out technique based on FIB machining gives high positional specificity,[18] so we employed it to prepare cross-sections of individual IBID-Pt contacts for cross-sectional TEM imaging (see Experimental for details).

Figures 1a,b are a typical pair of cross-sectional images obtained from the pristine nanowire segment away from the

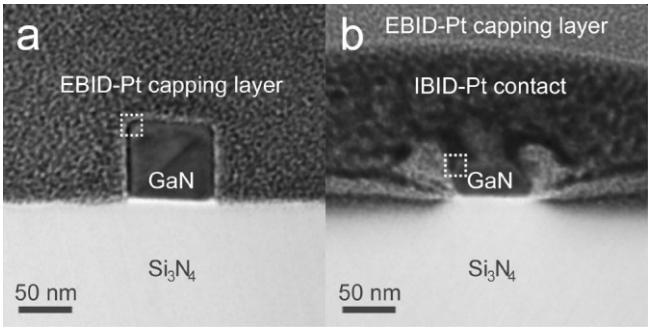

Figure 1. Bright-field scanning TEM (STEM) cross-sectional images of two points along a nanowire circuit. a) The pristine GaN nanowire is ~70 nm wide, and contains a twinning defect that will be discussed in a separate paper. In the EBID-Pt layer atop the nanowire, dark Pt nanocrystals were embedded in a bright amorphous C matrix. b) The contact region. The top ~30 nm of the nanowire has been sputtered away during IBID-Pt contact formation. Deposits of a bright, low-density material flank the nanowire on either side, reflecting inhomogeneity within the IBID-Pt contact. The IBID-Pt contact contains a higher density of Pt crystallites and appears darker than the EBID-Pt layer.

[*] Prof. J. E. Fischer, D. Tham, C.-Y. Nam
Department of Materials Science and Engineering
University of Pennsylvania
3231 Walnut Street, Philadelphia, PA 19104-6272 (USA)
E-mail: fischer@seas.upenn.edu

[**] This research was supported by the US Department of Energy Grant DE-FG02-98ER45701. The use of shared facilities supported by Penn's NSF/MRSEC under Grant DMR02-03378 is gratefully acknowledged.

contacts, and the FIB-contacted region, respectively. In Figure 1a, the crystalline GaN nanowire atop the Si_3N_4 substrate appears to be undamaged by the EBID-Pt capping layer. This suggests that EBID-Pt deposition is a benign process, which is corroborated by high-resolution TEM (HRTEM) images discussed further below. In Figure 1b, the IBID-Pt contact is comprised of denser material than the protective EBID-Pt capping layer and thus appears darker in bright-field scanning TEM (STEM) images. About 30 nm of the nanowire was sputtered off during deposition. The remaining part of the nanowire is flanked on either side by material less dense (bright areas) than the surrounding contact material (dark areas). The darkest and densest parts of the IBID-Pt contact were often directly atop the nanowire itself. Under the IBID-Pt contact, ~10 nm of the substrate was sputtered away and replaced with a dark and dense material. Dark, spotty contrast from a dense impregnated phase could be seen on either side of the nanowire as much as 50 nm beneath the substrate surface, but was absent directly beneath the nanowire. This suggests that, under our experimental conditions, the characteristic length for ion-beam damage is on the order of ~50 nm. Though not shown here, voids could sometimes be seen in the contact cross-sections because of incomplete IBID-Pt deposition under nanowire overhangs. Clearly, IBID-Pt deposition does not merely result in the formation of an IBID-Pt layer over the nanowire. Rather, it is a dynamic process whereby material irradiated by the ion beam is removed by sputtering as IBID-Pt is being deposited simultaneously. We emphasize that the contact regions of all nanowire circuits exhibited broadly similar morphologies for all nanowires ranging between 50 and 200 nm in diameter under the deposition conditions that we used for the IBID-Pt contacts.

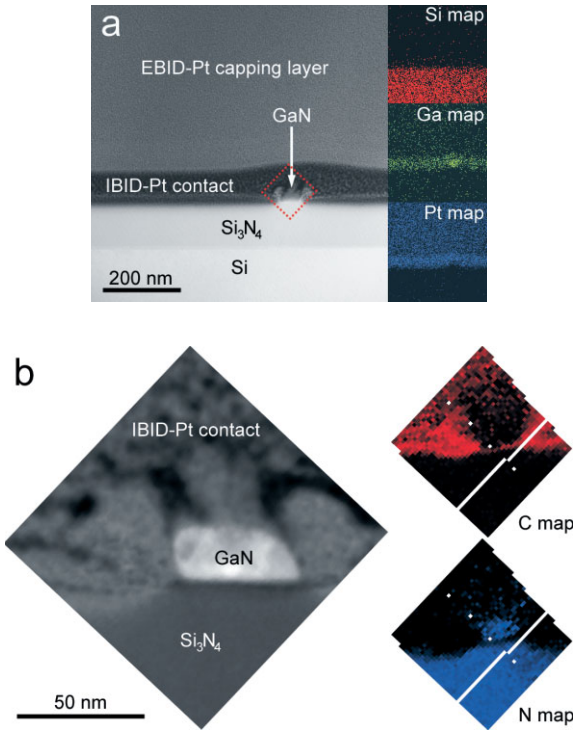

Figure 2. a) Bright-field STEM image of the cross-section in Figure 1b. Inset on the right shows X-ray elemental maps obtained from this region, obtained using characteristic X-rays from each element (Si K, Ga L, and Pt M X-rays). b) Dark-field STEM image of the region within the dashed box in (a). Insets on the right are electron energy-loss elemental maps from this region, obtained using characteristic energy-loss edges from each element (C K and N K edges). Missing data is due to sample drift.

Within the EBID-Pt capping layer and IBID-Pt contact, dark spotty contrast within a bright matrix suggested that dense Pt nanocrystallites were embedded within a low-density C matrix. This was corroborated later by X-ray energy dispersive spectroscopy (XEDS). Furthermore, electron energy-loss spectroscopy (EELS) showed that this matrix was composed mainly of amorphous C (not shown).

X-ray mapping was used to study the distribution of the heavier elements Si, Ga, and Pt. The bright-field STEM image in Figure 2a shows the nanowire covered by the dark and dense IBID-Pt contact on the substrate, with a brighter and less-dense EBID-Pt capping layer atop the IBID-Pt contact. The Pt X-ray map showed that both the IBID-Pt contact and EBID-Pt capping layers contain Pt, although the Pt density within the IBID-Pt contact is much higher. In addition, a bright band in the Ga X-ray map could be seen, indicating that Ga from the ion beam had been inadvertently incorporated into the IBID-Pt contact, as reported previously.[19] The GaN nanowire appears as a bright patch within this bright band in the Ga X-ray map. The Si map shows that Si was only found within the Si-containing substrates.

Low X-ray fluorescence yields and the limited energy resolution of the XEDS spectrometer (~145 eV) did not allow X-ray mapping of the light elements, C, N, and O. It was necessary to use EELS to map the distribution of these light elements. Figure 2b shows a dark-field STEM image of the region within the dashed box in Figure 2a. Elemental maps for C and N obtained from this region using EELS imaging are shown in the inset on the right. These maps have been divided by a featureless image taken at low loss and integrated over an identical energy width, to correct for modulations in intensity due to elastic scattering.[20,21] The low-density materials on either side of the nanowire are comparatively richer in C and poorer in Pt. These flanking deposits form during IBID-Pt deposition because hydrocarbon residues pile up along the sides of the nanowire after they are produced in adjacent regions via ion-beam-induced decomposition of the organometallic vapor. Though not shown here, O was occasionally detected in the space between the nanowire and the substrate, and we attribute this to entrapped water vapor.

HRTEM images of the pristine GaN nanowire within the region marked by the dashed box in Figure 1a confirm that there was no loss of GaN crystallinity at the interface with the EBID-Pt capping layer (see Fig. 3a). Therefore, EBID-Pt deposition does not affect the underlying material structure. While the GaN lattice contrast was occasionally smeared out due to damage during the thinning process (e.g., box labeled "c" in Fig. 3a), the level of disorder introduced was not read-

ADVANCED MATERIALS

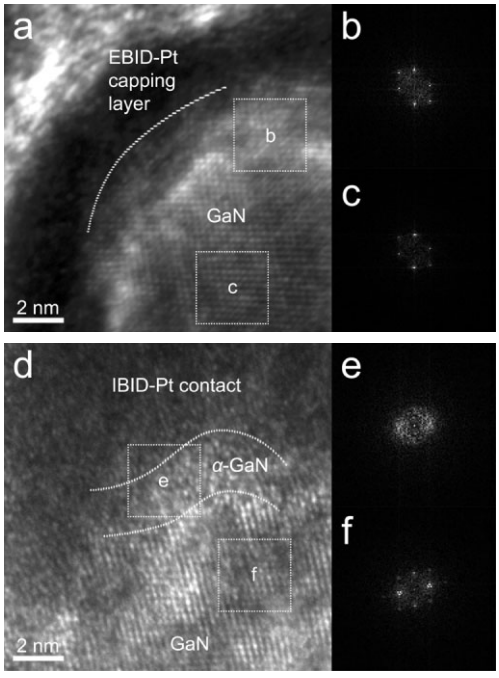

Figure 3. a) HRTEM image obtained from the region within the dashed box in Figure 1a. The interface between the GaN nanowire and the EBID-Pt capping layer is marked with a dashed line. Two boxes (b,c) are marked. b) Fast Fourier transform (FFT) diffractogram of the GaN region box labeled b. c) FFT diffractogram of the GaN region in the box labeled c. Sharp spots in both diffractograms show the high crystallinity of the nanowire all the way out to the interface. d) HRTEM image obtained from the region within the dashed box in Figure 1b. An amorphous GaN region (α-GaN) is marked between dashed lines. Two boxes (e,f) are marked. e) FFT diffractogram of the α-GaN region in box e, showing a diffuse-ring characteristic of amorphous material. f) FFT diffractogram of the GaN region in box f, with diffused disks, indicative of a disordered crystalline lattice.

ily noticeable in fast Fourier transform (FFT) diffractograms (Figs. 3b,c). Hence, we are convinced that no artifacts were introduced during the FIB lift-out process, and that the technique is sufficiently robust for HRTEM studies of the cross-sectional structure.

HRTEM images of the IBID-Pt/GaN nanowire contact were acquired along the entire contact interface. One such image, from the region marked by the dashed box in Figure 1b, is shown in Figure 3d. The IBID-Pt contact is the dark band across the top half of the image, with the crystalline GaN lattice below. Along the IBID-Pt contact interface, an amorphous GaN (α-GaN) region about 2–3 nm thick was visible between the dashed lines in Figure 3d. FFT diffractograms of this region show only a diffuse ring of intensity (Fig. 3e), confirming that the material is amorphous. Further below the interface, small isolated pockets of material suffered significant lattice damage and are visible as dark regions with smeared lattice contrast. FFT diffractograms from these regions showed enlarged diffuse spots, as in Figure 3f, indicating that the GaN lattice periodicity was degraded but not completely destroyed. For comparison, the FFT diffractograms in Figures 3b,c have much sharper spots, indicating significantly higher crystal quality in the pristine nanowire. These pockets of disordered GaN were not confined to the region immediately beneath the IBID-Pt contact interface, but were still visible near the GaN/substrate interface ~20 nm beneath the contact. Clearly, the deposition of an IBID-Pt layer does not completely protect the underlying nanowire from ion-beam damage. Nonetheless, it afforded sufficient protection against the large-scale amorphization reported for direct ion-beam irradiation studies on GaN nanowires.[22,23] At the same time, this finding also vindicates our initial choice of using EBID-Pt capping layers, which did not result in alteration of the underlying microstructure.

Our observations provide several explanations as to why FIB-deposited IBID-Pt forms unusually low-resistance ohmic contacts on GaN nanowires. The first reason for the low contact resistance is attributed to the low lead resistance, since IBID-Pt layers are known to have metal-like conductivity and low intrinsic resistivity.[10,13,24] Second, the presence of Ga in the IBID-Pt layer suggests that a work-function match is responsible for the low contact resistance: the Schottky-barrier height of Ga on n-GaN is only 0.1 eV. Third, the discovery of an amorphized GaN region underneath the contact suggests that Fermi-level pinning by interface states might be responsible for the low-resistance contact. Although the stoichiometry was not investigated, we also expect N vacancies to be formed after ion-beam irradiation.[22] Because amorphized GaN and N vacancies[25,26] are localized states that have energies around the conduction-band edge, Fermi-level pinning by these states can result in a low Schottky-barrier height and a low-resistance contact, because no deep mid-gap states exist in α-GaN.[27]

In our previous report on IBID-Pt-contacted GaN nanowire devices, the onset of linear current–voltage (I–V) characteristics was observed as the nanowire diameter decreased.[9] The identified ion-beam-induced amorphization of the GaN nanowire during the IBID-Pt process could explain this phenomenon via the increased fraction of amorphization underneath the contact region. Recall that the thickness of the amorphized region under the contact is almost identical for all diameters because of the identical deposition conditions. Since the surface/interface area of the amorphized region decreases with decreasing diameter, the amorphized volume fraction consequently increases, since the nanowire surface-to-volume ratio is proportional to inverse diameter. I–V measurements at different temperatures, T, (not shown) consistently showed variable-range hopping[28] conduction in contacts to small-diameter nanowires, confirming the importance of the amorphized region underneath the contact. Detailed I–V–T analysis will be published elsewhere.[29]

In summary, the morphological, compositional, and structural features of FIB-deposited IBID-Pt contacts to GaN nanowires have been elucidated for the first time. The results show that the contact-formation process results in a compositionally and structurally inhomogeneous contact region with a distinctive morphology. The general features of these low-re-

sistance contacts were insensitive to the choice of deposition conditions within the parameter space probed in this work, suggesting that this technique of contacting nanowires has a good tolerance for process variations. The IBID-Pt contacts were found to contain nanocrystalline Pt embedded in an amorphous matrix of C and Ga, and are already known to have metal-like conductivity and low intrinsic resistivities. An ~2–3 nm amorphous interface was visible in the HRTEM images of the contact interface, and this implied the creation of interface states that could pin the Fermi level within the nanowire. These characteristics of IBID-Pt contacts explain why they exhibit low contact resistances and low Schottky-barrier heights. We believe that these favorable contact properties are not limited to GaN nanowires, and that this technique will be applicable to a wide variety of nanowire materials. With a broader exploration of different deposition conditions, the thickness of the amorphous interfacial layer, as well as the level of local disorder, can be tuned, thereby enabling precise control of nanowire-contact properties.

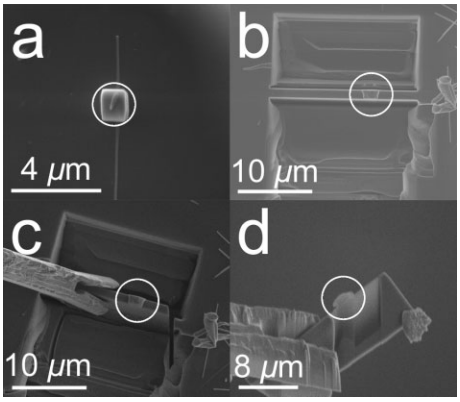

Figure 4. The FIB lift-out technique. The target area is circled in all four images. a) The target area is protected with a EBID-Pt capping layer. b) Trenches are cut on both sides of the target area. c) The micromanipulator is used to pick up the slab for further thinning. d) A side view of the slab shows that thinning has made the target area almost electron transparent.

Experimental

The n-type GaN nanowires used for this work were synthesized by thermal vaporization of Ga_2O_3 under an NH_3 atmosphere using a sputter-deposited AuPd film as the vapor–liquid–solid (VLS) catalyst [30]. After growth, the GaN nanowires were dispersed onto Si chips covered with 100 nm of Si_3N_4 or SiO_2. Using 30 keV Ga^+ ions in a dual-beam FIB (FEI Strata DB235), the IBID-Pt contacts were deposited on GaN nanowires with 50–200 nm diameters using 1–30 pA ion-beam currents, while maintaining a total ion dose of $\sim 6 \times 10^{16}$ cm^{-2} by varying the deposition time and pattern area. The corresponding nominal thickness of the contacts was 50 nm. These conditions are identical to those used in our previous report [9]. Two-probe *I–V* measurements were then made on these nanowire circuits, which exhibited low contact resistances and displayed a nonlinear response for thick nanowires with diameters greater than ~100 nm, but a linear response for thinner nanowires [9].

After *I–V* measurements were completed, the nanowire circuits were again loaded into the FIB. Multiple cross-sections from each nanowire circuit were obtained using the FIB. One cross-section was obtained from the pristine nanowire far away from both IBID-Pt contacts, while another cross-section was obtained from either of the two ion-beam-induced deposited Pt (IBID-Pt) contacts.

The cross-sections were produced by the lift-out technique, which has been described in detail elsewhere [18]. First, a region of interest was selected upon which a protective "capping layer" of Pt was deposited by EBID (Fig. 4a). EBID does not damage the underlying nanowire. This layer serves to protect the target region from inadvertent milling. The rate of EBID-Pt deposition was slow and therefore only small patterns were practical. In our experiments using 5 keV electrons, ~1 μm × 1 μm × 1 μm EBID-Pt capping layers were deposited in 30 min. In all cases, we did not expose the nanowire circuits to the ion beam until after ~1 μm thick protective EBID-Pt capping layers had been deposited over all the target sites.

Next, 20 μm long by 10 μm wide by 5 μm deep trenches on either side of the target region were milled away using the ion beam, to expose a ~1 μm thick slab (Fig. 4b). A micromanipulator within the FIB (Ascend Instruments Xtreme Access) was extended to grip the target slab, and the slab was cut free from the substrate using the ion beam (Fig. 4c). The target slab was then manipulated using the micromanipulator controls to distance it from the substrate. Further thinning of the slab to electron transparency was performed with progressively smaller ion-beam currents, beginning with 1000 pA and ending with 30 pA (Fig. 4d). The thinning was performed parallel to the cross-sectional plane to sequentially mill away the opposing surfaces. By milling parallel to the cross-sectional plane, the specimen–beam interaction depth was reduced [31], and damage to the region of interest was minimized. Cross-sections with thicknesses of ~100–200 nm were obtained, although the exact thickness was difficult to control. Nonetheless, EELS measurements of cross-sectional thickness in regions of identical composition showed that the surfaces were very flat, and the standard deviation of the thickness variations never exceeded 3 %.

After lift-out, the cross-sections were loaded into a 197 keV transmission electron microscope (JEOL 2010F) equipped with X-ray energy dispersive spectroscopy (XEDS, PGT-IMIX), and EELS (Gatan Imaging Filter) spectrometers. The cross-sections were carefully tilted to image them along the nanowire-growth direction. Using a 1 nm STEM probe, XEDS and EELS spectra were recorded from the cross-sections for compositional microanalysis. For all EELS work, the beam convergence angle and collection angle were 6.8 and 7.7 mrad, respectively. X-ray maps were acquired to map the distribution of elements Si, Ga, and Pt, using the Si K, Ga L, and Pt M characteristic X-rays. EELS images were acquired over the same specimen locations to map the distribution of light elements such as C, N, and O, using the C K, N K, and O K characteristic energy-loss edges. Finally, energy-filtered HRTEM images were acquired from the cross-sections using the EELS spectrometer to filter out inelastically scattered electrons.

Received: August 31, 2005
Final version: October 31, 2005
Published online: December 14, 2005

[1] S. Nakamura, S. Pearton, G. Fasol, *The Blue Laser Diode*, Springer, Berlin **2000**, p. 368.
[2] H. Yu, J. Li, R. A. Loomis, L.-W. Wang, W. E. Buhro, *Nat. Mater.* **2003**, *2*, 517.
[3] T. Uenoyama, *Phys. Rev. B* **1995**, *51*, 10 228.
[4] Y. Huang, C. M. Lieber, *Pure Appl. Chem.* **2004**, *76*, 2051.
[5] F. Qian, Y. Li, S. Gradecak, D. Wang, C. J. Barrelet, C. M. Lieber, *Nano Lett.* **2004**, *4*, 1975.
[6] P. Yang, *MRS Bull.* **2005**, *30*, 85.
[7] Y. Huang, X. Duan, Y. Cui, C. M. Lieber, *Nano Lett.* **2002**, *2*, 101.
[8] S. Jin, D. Whang, M. C. McAlpine, R. S. Friedman, Y. Wu, C. M. Lieber, *Nano Lett.* **2004**, *4*, 915.

[9] C. Y. Nam, J. Y. Kim, J. E. Fischer, *Appl. Phys. Lett.* **2005**, *86*, 193 112.
[10] G. D. Marzi, D. Iacopino, A. J. Quinn, G. Redmond, *J. Appl. Phys.* **2004**, *96*, 3458.
[11] V. Gopal, E. A. Stach, V. R. Radmilovic, *Appl. Phys. Lett.* **2004**, *85*, 49.
[12] S. B. Cronin, Y.-M. Lin, O. Rabin, M. R. Black, J. Y. Ying, M. S. Dresselhaus, P. L. Gai, J.-P. Minet, J.-P. Issi, *Nanotechnology* **2002**, *13*, 653.
[13] J.-F. Lin, J. P. Bird, L. Rotkina, P. A. Bennett, *Appl. Phys. Lett.* **2003**, *82*, 802.
[14] A. N. Bright, C. J. Humphreys, *Philos. Mag. B* **2001**, *81*, 1725.
[15] A. N. Bright, P. J. Thomas, M. Weyland, D. M. Tricker, C. J. Humphreys, *J. Appl. Phys.* **2001**, *89*, 3143.
[16] S. B. Newcomb, C. B. Boothroyd, W. M. Stobbs, *J. Microsc.* **1985**, *140*, 195–207.
[17] D. B. Williams, C. B. Carter, *Transmission Electron Microscopy*, Plenum Press, New York **1996**, p. 703.
[18] L. A. Giannuzzi, J. L. Drown, S. R. Brown, R. B. Irwin, F. A. Stevie, *Microsc. Res. Tech.* **1998**, *41*, 285.
[19] L. Rotkina, J.-F. Lin, J. P. Bird, *Appl. Phys. Lett.* **2003**, *83*, 4426.
[20] R. F. Egerton, *Ultramicroscopy* **1978**, *3*, 243.
[21] J. H. Butler, F. Watari, A. Higgs, *Ultramicroscopy* **1982**, *8*, 327.
[22] S. Dhara, A. Datta, C. T. Wu, Z. H. Lan, K. H. Chen, Y. L. Wang, Y. F. Chen, C. W. Hsu, L. C. Chen, H. M. Lin, C. C. Chen, *Appl. Phys. Lett.* **2004**, *84*, 3486.
[23] S. Dhara, A. Datta, C. T. Wu, Z. H. Lan, K. H. Chen, Y. L. Wang, L. C. Chen, C. W. Hsu, H. M. Lin, C. C. Chen, *Appl. Phys. Lett.* **2003**, *82*, 451.
[24] J.-F. Lin, J. P. Bird, L. Rotkina, *Physica E* **2003**, *19*, 112.
[25] D. C. Look, G. C. Farlow, P. J. Drevinsky, D. F. Bliss, J. R. Sizelove, *Appl. Phys. Lett.* **2003**, *83*, 3525.
[26] T. Hashizume, R. Nakasaki, *Appl. Phys. Lett.* **2002**, *80*, 4564.
[27] P. Stumm, D. A. Drabold, *Phys. Rev. Lett.* **1997**, *79*, 677.
[28] N. F. Mott, *Conduction in Non-crystalline Materials*, Clarendon Press, Oxford, UK **1993**, p. 128.
[29] C. Y. Nam, D. Tham, J. E. Fischer, *Nano Lett.* **2005**, *5*, 2029.
[30] C. Y. Nam, D. Tham, J. E. Fischer, *Appl. Phys. Lett.* **2004**, *85*, 5676.
[31] B. I. Prenitzer, C. A. Urbanik-Shannon, L. A. Giannuzzi, S. R. Brown, R. B. Irwin, T. L. Shofner, F. A. Stevie, *Microsc. Microanal.* **2003**, *9*, 216.

